

Delafossite oxides ABO_2 ($A = \text{Ag, Cu; } B = \text{Al, Cr, Fe, In, Nd, Y}$) studied by perturbed-angular-correlation spectroscopy using a $^{111}\text{Ag}(\beta^-)^{111}\text{Cd}$ probe

R. N. Attili,* R. N. Saxena, A. W. Carbonari, and J. Mestnik Filho

Instituto de Pesquisas Energéticas e Nucleares, CP 11049, CEP 05422-970 São Paulo, SP, Brazil

M. Uhrmacher and K. P. Lieb

II. Physikalisches Institut der Universität Göttingen, Bunsenstrasse 7-9, D-37073 Göttingen, Germany

(Received 10 February 1998; revised manuscript received 6 April 1988)

The electric-field gradient (EFG) at ^{111}Cd nuclei dilutely substituting an A cation site in delafossites $A^{+1}B^{+3}O_2$ has been measured using a perturbed-angular-correlation technique. The radioactive isotope $^{111}\text{Ag}(\beta^-)^{111}\text{Cd}$ was used as the hyperfine probe and introduced into the samples by thermal diffusion. The EFG's measured using a $^{111}\text{Ag} \rightarrow ^{111}\text{Cd}$ probe are compared with those measured using the $^{111}\text{In} \rightarrow ^{111}\text{Cd}$ probe and with the calculated values using the point-charge model including the local distortion introduced by the probe. The results are also discussed in terms of a previously observed correlation between the electric-field gradient and the cation-oxygen bond length in these delafossites and other binary oxides.

[S0163-1829(98)01329-0]

I. INTRODUCTION

Properties of solids such as magnetic order, electronic structure, structural phase transitions, defects, and chemical bonding are often studied by means of the perturbed-angular-correlation (PAC) method via the hyperfine interaction of radioactive probe nuclei with their electronic environment. The local oxygen configuration around the cation site in many binary and ternary metal oxides (A_2O_3 and $A_2Cu_2O_5$) has been studied in a systematic manner by PAC (Refs. 1 and 2) using an $^{111}\text{In}(\text{EC})^{111}\text{Cd}$ probe. These investigations revealed a correlation between the electric-field gradient (EFG) at ^{111}Cd probe nuclei on a substitutional cation site and parameters like the ionic radius of the cation and the cation-oxygen bond length. Similar studies have been carried out recently on delafossite oxides ABO_2 , extending the earlier systematics.³ In this context the delafossite oxides provided an interesting comparison: while the basic crystal structure remains the same, the ionic radii of the B element in these compounds cover a much larger range than the previously studied binary and ternary oxides.

Delafossites $A^{+1}B^{+3}O_2$ crystallize in a hexagonal layered structure that belongs to the space group $R\bar{3}m$ or $P6_3/mmc$ (Fig. 1). The trivalent ions B^{+3} are located at the center of regular oxygen octahedra that are inclined and connected by monovalent ions A^{+1} . The $R\bar{3}m$ hexagonal delafossites contain three ABO_2 molecules per unit cell and have lattice constants a and c ranging from 2.8 to 3.8 Å and 17 to 19 Å, respectively.

The hexagonal description can also be viewed as a sequence of planes with different ions in the order $O^{-2}-B^{+3}-O^{-2}-A^{+1}-O^{-2}-B^{+3}-O^{-2}$, forming two-dimensional triangular lattices. In the family $A^{+1}B^{+3}O_2$, A can be Cu, Ag, Pd, and Pt while B is Al, Ga, In, Sc, Y, Cr, Fe, rare earths, etc. These compounds exhibit a variety of interesting properties. The Cu- and Ag-based compounds are semiconductors, while Pt- and Pd-based compounds are conductors.⁴ The compounds

CuFeO_2 , CuCrO_2 , and AgCrO_2 are antiferromagnetic.^{5,6} The delafossite oxides thus present two distinct cation sites and, in hyperfine interaction studies with radioactive impurity probes, each of these two sites can be occupied by the probe atoms.

In the previous PAC study,³ the electric-field gradient of $^{111}\text{In}(\text{EC})^{111}\text{Cd}$ nuclei in delafossites $A^{+1}B^{+3}O_2$ ($A = \text{Ag, Cu; } B = \text{Al, Cr, Fe, In, Nd, Y}$) was measured. For each compound at least one EFG with axial symmetry was found, which was attributed to ^{111}In probes on the substitutional B site. The assignment of the probe site location was based mainly on chemical arguments that suggest a preference for

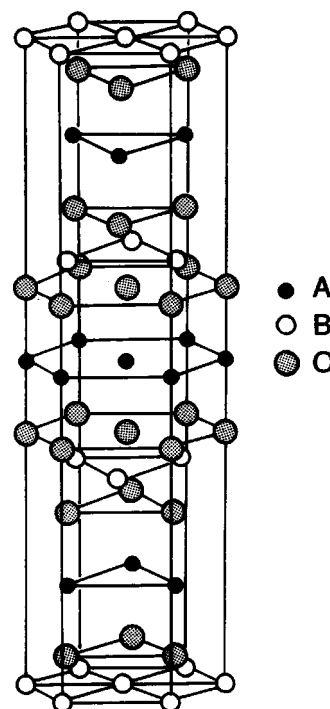


FIG. 1. Delafossite structure ($R\bar{3}m$).

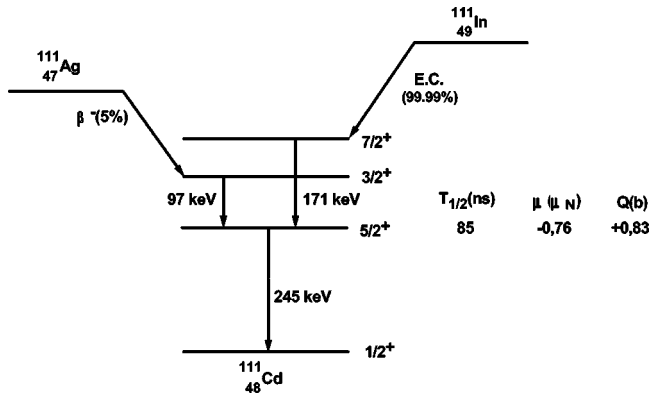


FIG. 2. Simplified decay scheme of ^{111}In and ^{111}Ag . The values of magnetic moment (μ) and quadrupole moment (Q) are taken from compilations in Refs. 8 and 10, respectively.

the ^{111}In probe for a trivalent cation site. PAC, conversion electron Mössbauer spectroscopy measurements in CuFeO_2 , and low-temperature PAC measurements of CuFeO_2 , CuCrO_2 , and AgCrO_2 (Ref. 7) provided additional support, although indirectly, for the B site localization of the ^{111}In probes. The measured EFG's for ^{111}Cd at the B site³ show a relatively weak temperature dependence and cannot be reproduced with the simple point-charge model (PCM) calculations, except for the case of AgInO_2 . The authors attributed this observation to the partially covalent character of chemical bonding in these compounds.

In the present work we report on the systematic study of EFG's in all the delafossite oxides studied previously,³ now using radioactive ^{111}Ag probes that decay via the β^- process to the same hyperfine-interaction-sensitive level in ^{111}Cd as the ^{111}In probe nuclei employed in the previous work. However, on the basis of the different chemical nature of Ag, one expects them to occupy A cation sites that are bonded to oxygen neighbors in a linear chain (see Fig. 1). The radioactive decay of ^{111}Ag and ^{111}In proceeds through the 245 keV $5/2^+$ state in ^{111}Cd having the half life $T_{1/2} = 85$ ns, quadrupole moment $Q = 0.83(14)$ b , and magnetic moment $\mu = -0.76\mu_N$, as displayed in Fig. 2.⁸

This particular feature of two radioactive parent atoms with quite different chemical nature but decaying to same hyperfine probe level, provides an interesting situation and directly leads to an unambiguous information with regard to the site location of the probes in this class of ternary oxides. Another motivation for the present work was to compare the EFG measured after thermal diffusion of ^{111}In (and ^{111}Ag) probes with those obtained after ^{111}In ion implantation and subsequent annealing of the radiation-induced lattice damages.

II. EXPERIMENTAL PROCEDURE

The delafossite oxides samples used in the present investigation were prepared at the University of Göttingen where part of the samples had been used in the earlier PAC experiments³ with ion-implanted ^{111}In . In the present study, the compounds AgCrO_2 , AgInO_2 , CuAlO_2 , CuCrO_2 , CuFeO_2 , CuNdO_2 , and CuYO_2 were measured using ^{111}Ag probes. In order to check for any possible differences be-

tween the present experiment, where the radioactive ^{111}Ag is introduced into the sample by thermal diffusion, and the previous results,³ where ^{111}In nuclei were ion implanted into the samples, the compounds CuNdO_2 and CuYO_2 were also measured using thermally diffused ^{111}In .

Both ^{111}Ag and ^{111}In probes were introduced into the oxide samples by thermal diffusion at 1073 K. The carrier-free ^{111}In was obtained from Nordion International Inc. in the form of a dilute InCl_3 solution. The radioactive solution containing carrier-free ^{111}Ag was prepared at IPEN, São Paulo, from the decay of $^{111m,g}\text{Pd}$, which was produced by the nuclear reaction $^{110}\text{Pd}(n, \gamma)^{111m,g}\text{Pd}$. About 100 mg of natural Pd metal were irradiated in a thermal neutron flux of 10^{13} n/cm^2 s for about 40 h in the IEA-R1 nuclear reactor at IPEN. The isotopes ^{111m}Pd and ^{111g}Pd have short half-lives (5.5 h and 22 min, respectively) and eventually decay to ^{111}Ag . The radioactive isotope ^{111}Ag has a half-life of 7.45 days and beta decays to the excited states of the ^{111}Cd as shown in Fig. 2.

Carrier-free ^{111}Ag was obtained by chemically separating Ag from the Pd after neutron irradiation. The irradiated Pd was dissolved in a small volume of aqua regia. The solution was evaporated to complete dryness and taken up in 12M HCl. This solution was then loaded on top of a column containing Bio-Rad AG 1-X8 (100 mesh) anion exchange resin preconditioned with concentrated HCl. The silver activity was washed off the column with a solution of concentrated HCl while Pd remained on the column under this condition. A few drops of concentrated HNO_3 were added to the collected solution and it was evaporated to complete dryness. The conical Pyrex tube containing ^{111}Ag was then rinsed with a couple of drops of distilled water. Part of this solution was deposited on the delafossite oxide sample that was dried under an infrared lamp. The activity was diffused into the samples by heating in a resistance furnace at 1073 K during 24 h in a N_2 flux. The same procedure was adopted for thermal diffusion of the ^{111}In activity into the CuNdO_2 and CuYO_2 samples.

The PAC method is based on the hyperfine interaction of nuclear moments with extra nuclear magnetic fields or EFG's. A detailed description of this method can be found in Ref. 9. In the case of electric quadrupole interaction, the perturbed time-differential γ - γ angular correlation can be expressed (neglecting the A_{44} term) as

$$W(\theta, t) = 1 + A_{22}G_{22}(t)P_2(\cos \theta), \quad (1)$$

where θ denotes the angle between the detectors, A_{22} the unperturbed angular correlation coefficient of the γ - γ cascade, and $P_2(\cos \theta)$ the Legendre polynomial. The perturbation factor $G_{22}(t)$ contains detailed information about the hyperfine interaction. In case of a static quadrupole interaction in a polycrystalline sample and the nuclear level with spin $I = \frac{5}{2}$, the perturbation factor is expressed as

$$G_{22}(t) = S_{20} + \sum_{n=1}^3 S_{2n} \cos(\omega_n t) \exp(-\omega_n^2 \tau_R^2 / 2) \\ \times \exp(-\omega_n^2 \delta^2 t^2 / 2), \quad (2)$$

where the amplitudes S_{2n} and frequencies ω_n depend on the nuclear quadrupole frequency

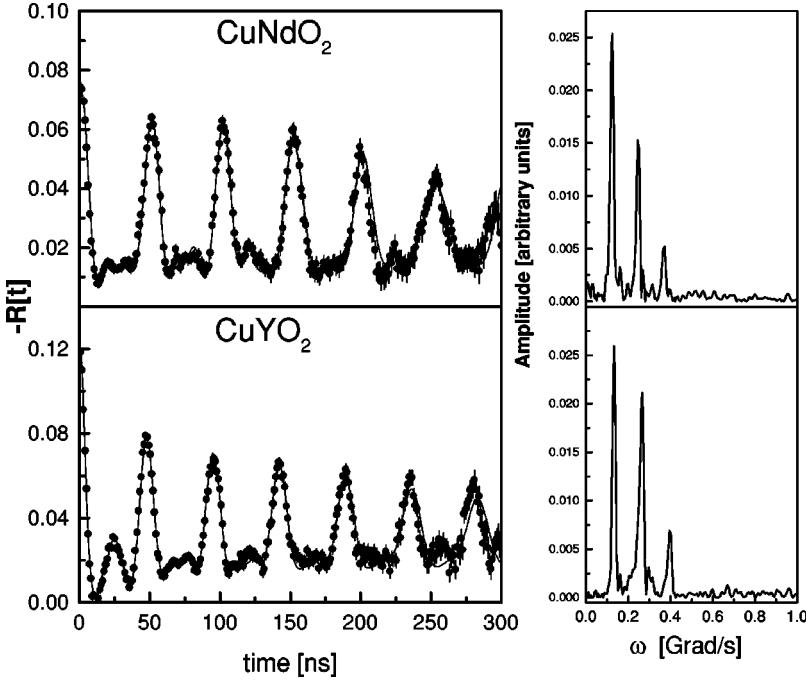


FIG. 3. PAC spectra and the corresponding Fourier transform for $^{111}\text{In} \rightarrow ^{111}\text{Cd}$ in delafossites at room temperature.

$$\omega_Q = \frac{eQV_{zz}}{4I(2I-1)\hbar} \quad (3)$$

and the asymmetry parameter defined as

$$\eta = \frac{V_{yy} - V_{xx}}{V_{zz}} \quad (4)$$

with $0 \leq \eta \leq 1$. As usual, V_{zz} is the principal component of the EFG tensor.

The terms $\exp(-\omega_n^2 \tau_R^2/2)$ and $\exp(-\omega_n^2 \delta^2 t^2/2)$ take into account the effects of the finite time resolution of the detectors τ_R and the distribution of the EFG around a mean value with a width δ , respectively.

The experimental perturbation function $R(t)$ is calculated from the measured time spectra as follows:

$$R(t) = 2 \left[\frac{W(180^\circ, t) - W(90^\circ, t)}{W(180^\circ, t) + 2W(90^\circ, t)} \right] = A_{22} \sum_i f_i G_{22}^i(t) \quad (5)$$

and depends on the relative fractions f_i of different EFG's that contribute to the PAC spectrum with corresponding perturbation factors $G_{22}^i(t)$.

The PAC measurements were carried out with a conventional slow-fast coincidence setup consisting of four BaF_2 scintillation detectors. This setup permitted simultaneous acquisition of eight time-differential coincidence spectra. The time resolution of the system was about 0.8 ns for the gamma cascades 173–245 keV and 97–245 keV, which are populated in the decays of ^{111}In and ^{111}Ag , respectively. All the samples were measured at room temperature.

III. EXPERIMENTAL RESULTS

Results of the least-squares fit of the experimental PAC spectra to the function given by Eq. (2) for some of the delafossite samples studied are presented in Figs. 3 and 4

along with their Fourier transforms. The experimental parameters extracted from the analysis of the data are listed in Table I. For comparison, the results for the B site in each of these compounds, obtained in the earlier work,³ have also been included in this table. In this case only the values attributed to delafossite phases are shown. Using the value of $Q = 0.83(14)b$ (Ref. 10) for the nuclear quadrupole moment of the 245 keV state of ^{111}Cd , we obtained the experimental values of the V_{zz} presented in Table II. As observed for the B site,³ the asymmetry parameter η for the A site is also zero for all the compounds studied. This is, indeed, expected in view of the known point symmetry of both A and B atoms in the delafossite oxides.

The experimental data for most of the samples could be fitted to a single quadrupole frequency with very small ($\delta \sim 2\%$) distribution. However, in a few cases an additional EFG component, with less than 10–15% site population, was observed that was attributed to impurity phases, most probably binary metal oxides. This observation contrasts with the

TABLE I. Experimental hyperfine parameters for delafossite oxides.

Compound	^{111}Ag			$^{111}\text{In}^a$		
	ω_Q (Mrad/s)	δ (%)	η	ω_Q (Mrad/s)	δ (%)	η
CuAlO_2	86.5(0.4)	1.9(0.2)	0	23.6(0.4)	1.5	0
CuCrO_2	65.7(0.3)	2.3(0.2)	0	19.8(0.2)	4(1)	0
CuFeO_2	88.2(0.3)	0.6(0.2)	0	19.6(0.2)	0.5	0
CuNdO_2	66.1(0.3)	1.4(0.1)	0	22.0(0.6)	2.6	0
				20.8(0.1) ^b	2.5(0.1) ^b	0 ^b
CuYO_2	45.5(0.3)	1.1(0.1)	0	21.4(0.3)	2(1)	0
				22.2(0.1) ^b	2.2(0.1) ^b	0 ^b
AgCrO_2	83.9(0.3)	0.3(0.1)	0	20.6(0.2)	0.5	0
AgInO_2	98.8(0.4)	0	0	14.3(0.9)	4.4	0

^aReference 3.

^bThis work.

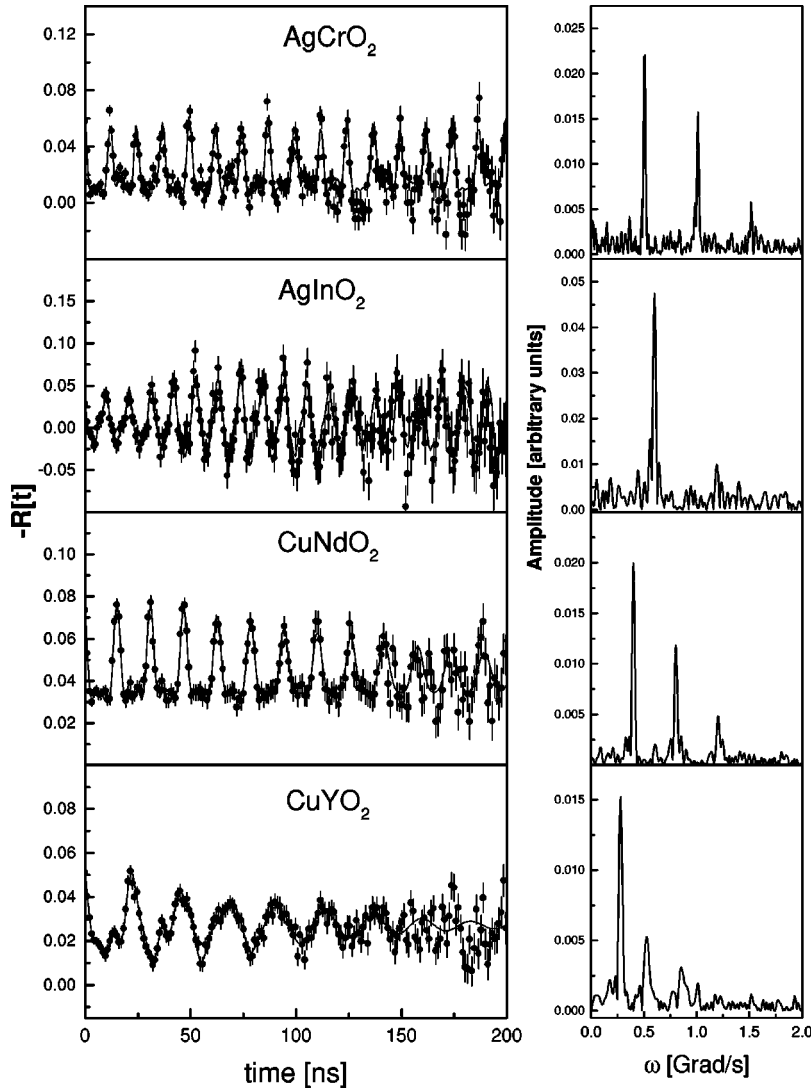


FIG. 4. PAC spectra and the corresponding Fourier transform for $^{111}\text{Ag} \rightarrow ^{111}\text{Cd}$ in delafossites at room temperature.

results obtained in Ref. 3 where the authors reported significant contributions of the impurity phases, some of them not completely identified. A predominantly single phase found in most of the samples in the present study most probably resulted from the higher temperature, and the longer annealing times, used during diffusion of the activities. We will not consider the minor phases in further analysis of the results.

Measurements in the CuYO_2 and CuNdO_2 samples were also carried out using ^{111}In probes in order to verify any

possible difference in the observed quadrupole interaction that could be attributed to the different methods used for incorporating the radioactive ^{111}In nuclei into the samples. The results presented in Table I show good agreement between the present results and those obtained after ^{111}In implantation. The result may be especially important to PAC work using ion-implanted samples, since it reinforces the generally accepted idea that despite the fact that ion implantation produces radiation damage of the crystal lattice, most

TABLE II. Experimental and calculated values of V_{zz} using PCM for *A* and *B* sites in delafossites.

Compound	^{111}Ag		^{111}In		<i>A</i> site		<i>B</i> site	
	$ V_{zz}^{exp} $ (10^{21} V/m 2)	η	$ V_{zz}^{exp} $ (10^{21} V/m 2)	η	V_{zz}^{PCM} (10^{21} V/m 2)	η	V_{zz}^{PCM} (10^{21} V/m 2)	η
CuAlO_2	27.44	0	7.47	0	-44.19	0	3.33	0
CuCrO_2	20.84	0	6.28	0	-44.80	0	3.03	0
CuFeO_2	27.96	0	6.21	0	-46.01	0	2.12	0
CuNdO_2	20.97	0	6.98	0	-47.52	0	11.81	0
CuYO_2^a	14.43	0	6.68	0	-46.92	0	10.60	0
AgCrO_2	26.62	0	6.53	0	-32.99	0	2.42	0
AgInO_2	31.34	0	4.53	0	-31.78	0	4.54	0

^a $P6_3/mmc$.

of it is annealed out by appropriate thermal treatment, and the impurity atoms relax into substitutional sites during annealing.

IV. DISCUSSION

A. Site location

One of the main motivations for this work was to determine the location of the radioactive probe atoms substituting host cations in the delafossite oxides. The quadrupole frequencies given in Table I and in particular those for AgInO_2 , where the probe atoms are not impurities, clearly show that the site of ^{111}Ag and ^{111}In are not the same, or else they would give rise to identical quadrupole frequencies since both parent nuclei eventually decay to ^{111}Cd for which the interaction is measured. In addition, the fact that we observe only a single quadrupole frequency with very small distribution in both cases indicates that the probe atoms are most likely placed at the substitutional sites. These observations therefore constitute a direct evidence that ^{111}Ag and ^{111}In atoms in fact substitute Ag and In sites, respectively, in AgInO_2 . Since the measured quadrupole frequencies for ^{111}Ag and ^{111}In in all the other delafossite oxides studied are likewise quite different, we conclude that we are dealing with different probe sites in these compounds and that the radioactive ^{111}Ag substitute the A atoms and ^{111}In substitute the B atoms in the oxides ABO_2 . This conclusion is obviously consistent with the expected chemical affinity of Ag and In for univalent and trivalent cations and strengthens the assignments of site location made in Ref. 3.

B. Comparison with the PCM

Theoretical predictions of the EFG for impurity atoms in a solid matrix are still a challenging problem. Very few detailed calculations involving band structures have been performed in oxides. Luthin *et al.* have recently reported¹¹ on cluster EFG calculations for ^{111}Cd in HfO_2 and ZrO_2 . The standard approach in the past therefore was to perform the calculation of EFG using the simple PCM. We have adopted this approach to calculate the values of V_{zz} and η both at the A and the B sites, using the usual lattice sum method. For these calculations, lattice parameters at room temperature were taken from literature¹²⁻¹⁹ to obtain the relevant coordinates of the ions. Formal charges of +1, +3, and -2 were assigned to A , B , and oxygen atoms, respectively. The lattice sum was performed numerically up to a distance of 70 Å from the probe nucleus. The resulting values of V_{zz}^{lat} were then multiplied by $(1 - \gamma_{\infty})$, where $\gamma_{\infty} = -29.27$ is the known²⁰ Sternheimer antishielding factor for Cd, to deduce the EFG at the nuclear site, V_{zz}^{PCM} . Table II lists the resulting values of V_{zz}^{PCM} and η in comparison with the measured parameters obtained with the ^{111}Ag and ^{111}In probes. The predicted and measured η values are in perfect agreement with each other at both sites. This is not the case for the calculated and measured values of $|V_{zz}|$, except for the AgInO_2 samples, where excellent agreement is found for both sites. The PCM overestimates the EFG at the A site in CuBO_2 by a factor of up to 3. For the B site the calculated values are underestimated by a factor of about 2-3 for

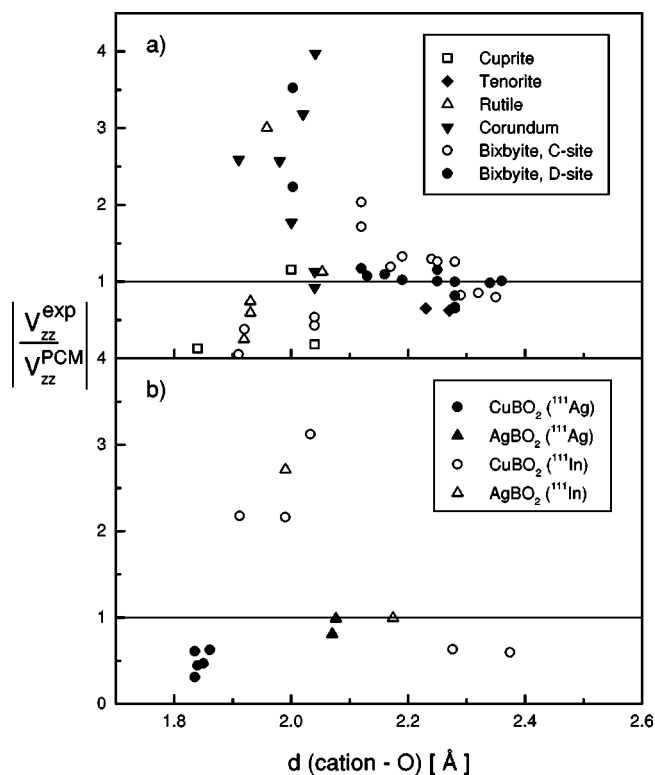


FIG. 5. The ratio $V_{zz}^{\text{exp}}/V_{zz}^{\text{PCM}}$ is plotted versus the bond length d (cation-O) in oxides (a) taken from the compilation in Ref. 21 and (b) for the A sites (present data) and B sites (data from Ref. 3) in delafossites.

CuAlO_2 , CuCrO_2 , CuFeO_2 , and AgCrO_2 but somewhat overestimated for CuYO_2 and CuNdO_2 .

Our method of analyzing the results is similar to that employed by Wiarda *et al.*²¹ and Attili *et al.*³ for ^{111}In in binary oxides and delafossites. Adding the present data for the A site to this systematics, in Fig. 5 we have plotted the ratio $|V_{zz}^{\text{exp}}/V_{zz}^{\text{PCM}}|$ versus the cation-oxygen bond length of the (undoped) matrices. It had been concluded that binary oxides with bond lengths exceeding 2.1 Å should have a predominantly ionic bonding, whereas those with bond lengths of less than 2.1 Å have a partially covalent bonding with both negative and positive contributions to the EFG. This leads to a splitting of the ratio $|V_{zz}^{\text{exp}}/V_{zz}^{\text{PCM}}|$ into two groups for small bond lengths.

Originally, this splitting was thought to be a consequence of the different crystal structures of the binary oxides. The B site EFG's in the delafossites showed a similar trend, but no splitting for small bond lengths was observed. Since the delafossites cover a wide range of cation-oxygen bond lengths from 1.912 Å to 2.374 Å, while the crystal structure remains the same, it was argued that, indeed, the cation-oxygen bond length is the decisive parameter responsible for the disagreement between the experimental and PCM values for the EFG's at shorter bond lengths. With the present data for the A site included in the systematics (see Fig. 5), we now have a second group of EFG's in delafossite oxides at bond lengths of < 2.1 Å that are smaller than predicted by the PCM. Bartos *et al.*¹ studied, via PAC with ^{111}In impurities, bixbyite oxides that exhibit two sites, labeled C and D sites, having identical valences. For ^{111}Cd on D sites in sev-

eral bixbyites, smaller EFG's than predicted by the PCM have been encountered (see Fig. 5). In contrast to this, the delafossites offer two sites with different valences, but they also show the splitting.

C. Distortion effects at the probe sites

One effect, which may strongly influence the quadrupole hyperfine interaction of an impurity probe atom, is the local distortion of the lattice introduced by the probe, particularly when the radioactive parent nucleus undergoes a transmutation via β processes or electron conversion leaving the daughter atoms on the corresponding lattice site(s) of the parent atom(s). This is the case of ^{111}Ag and ^{111}In decaying to ^{111}Cd . In most cases, the ionic size of Cd^{+2} differs from that of the host ion it replaces and may therefore cause a local distortion of the crystal lattice. Usually the PCM does not consider such distortion and for that reason may fail to reproduce the experimentally observed field gradients. PCM calculations including distortion have been carried out for example for ^{111}Cd in TiO_2 (Ref. 22) and, indeed, led to agreement with the experimental quadrupole interaction parameters.

In order to verify whether the deficiency of PCM for the *A* and *B* sites in delafossites can be explained by lattice distortion caused by the probe ion $^{111}\text{Cd}^{+2}$, we extended the PCM calculations by including the distortion of the nearest-neighbor oxygen ions. These were displaced from their equilibrium positions in such a way as to preserve axial symmetry around the probe in order to reproduce the experimentally observed values of $\eta=0$. Furthermore, the usual Sternheimer antishielding factor $\gamma_\infty = -29.27$ was adopted in the calculations.

A site cations in delafossite oxides are monovalent and have a twofold linear coordination parallel to the *c* axis. In the calculations, the two oxygen ions directly bonded to $^{111}\text{Cd}^{+2}$ were shifted from their equilibrium positions and the lattice sum was performed with these new coordinates to arrive at values of V_{zz}^{latt} and $V_{zz}^{dis} = V_{zz}^{latt}(1 - \gamma_\infty)$. The *B* cations in delafossites have a sixfold coordination of oxygen nearest neighbors in a trigonally distorted octahedral configuration characterized by D_{3d} point symmetry. The oxygen ions of this octahedron were displaced in a symmetric manner along the principal axes. Positive as well as negative shifts were allowed in the calculation. The resulting values of V_{zz}^{dis} as a function of shift are plotted in Fig. 6 for the Cu and Fe site in CuFeO_2 , as an example. The shifts necessary to achieve agreement with the experiment for each compound are listed in Table III. For the *A* site, in all the cases the shifts are positive as expected for oversized $^{111}\text{Cd}^{+2}$ ions. However, most shifts are unrealistically large and certainly would also affect the next-nearest and farther ions around the probes. Since the sign of V_{zz} is not determined in the PAC experiments, for *B* sites, both positive and negative shifts lead to agreement with the measured EFG's. However, taking into account the oversized Cd^{+2} ion, we should consider only positive shifts. As can be seen from Table III, the required shifts are again quite large in practically all the cases.

The results demonstrate that these simplifying assumptions do not lead to a realistic description of the data, and

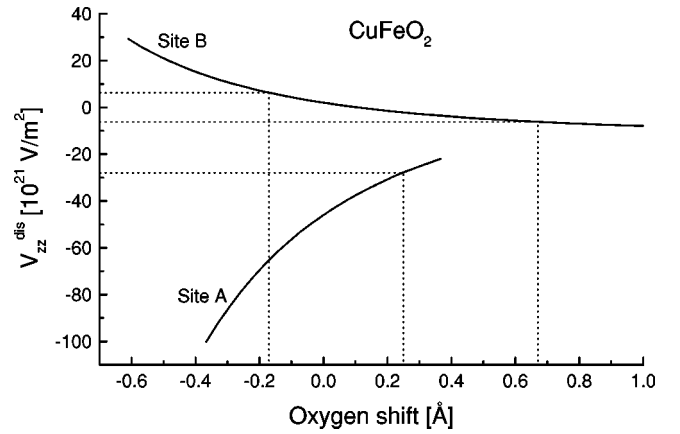


FIG. 6. PCM calculations of V_{zz} as a function of the first oxygen neighbor shifts around Cu^{+1} (site *A*) and Fe^{+3} (site *B*) ions in CuFeO_2 . The dashed lines show the corresponding experimental V_{zz} values for the *A* site and *B* site (positive and negative). The ionic equilibrium Cu-O and Fe-O distances in CuFeO_2 are 1.84 Å and 2.03 Å, respectively.

other effects such as covalent bonding cannot be ignored.^{15,23} To illustrate this point, we shortly comment on the results of the previous PAC experiment for the *B* site³ and the Mössbauer effect⁷ in the compound CuFeO_2 . Since the Mössbauer probe isotope ^{57}Fe is a host atom, it does not introduce any lattice distortion. The Mössbauer data give $V_{zz}^{exp} = 3.72 \times 10^{21} \text{ V/cm}^2$, corresponding to a lattice EFG of $V_{zz}^{latt} = 0.37 \times 10^{21} \text{ V/cm}^2$ if we use the Sternheimer factor $\gamma_\infty = -9.14$ (Ref. 24) of Fe. In a similar fashion, the PAC data gave $V_{zz}^{latt} = 0.21 \times 10^{21} \text{ V/cm}^2$. If we now compare these values with that predicted by the simple PCM, $V_{zz}^{latt} = 0.065 \times 10^{21} \text{ V/cm}^2$, we immediately notice that (a) in the case of the ^{57}Fe Mössbauer experiment there remains a large discrepancy by a factor of 5.6, in spite of the fact that no lattice distortion is expected, (b) in the case of the ^{111}Cd PAC experiment, where a lattice distortion is likely to occur, the discrepancy is less severe (≈ 3.2).

V. CONCLUSIONS

Electric-field gradients at ^{111}Cd impurities have been determined at the substitutional *A* site of the delafossite oxides (ABO_2) using the PAC method. The radioactive tracer

TABLE III. Isotropic oxygen shifts necessary to reproduce the experimental V_{zz} values for the *A* and *B* sites in delafossites.

Compound	<i>A</i> site Oxygen shift (Å)	<i>B</i> site	
		Isotropic shift for $+V_{zz}^{exp}$ (Å)	Isotropic shift for $-V_{zz}^{exp}$ (Å)
CuAlO_2	+0.25	-0.12	+0.73
CuCrO_2	+0.39	-0.13	+0.68
CuFeO_2	+0.25	-0.17	+0.67
CuNdO_2	+0.44	+0.28	+1.17
CuYO_2 ^a	+0.61	+0.11	+2.00
AgCrO_2	+0.13	-0.16	+0.70
AgInO_2	0	0	+0.93

^a $P6_3/mmc$.

$^{111}\text{Ag}(\beta^-)^{111}\text{Cd}$ used in the present investigation enabled definite identification of the probe location in these compounds. An analysis of the previous PAC results using the $^{111}\text{In}(\text{EC})^{111}\text{Cd}$ tracer, in conjunction with the present results, clearly shows that in these delafossites ^{111}Ag and ^{111}In radioactive atoms substitute A and B cation sites, respectively.

The experimental EFG's at the A site determined in the present investigation fit in well with the trend previously established for the B site in delafossites and in binary oxides.^{3,21} In these compounds the deviation of the measured EFG from the predictions of the PCM correlates with the cation-oxygen bond length. The present results are in agreement with the earlier suggestion³ that covalent bonding is most probably responsible for this deviation, although no quantitative explanation of the effect has been reached yet. PCM calculations of EFG's were also carried out, taking into account distortions caused by the probe impurity, in an attempt to remedy the discrepancy between the experimental

values and the PCM calculation. This was done by dislocating the positions of the nearest-neighbor oxygen ions around either the A or B cations and at the same time keeping the symmetry of the EFG. The calculations showed that in most cases unrealistically large shifts would be required to obtain agreement with experiment.

ACKNOWLEDGMENTS

This work was partially supported by CNPq (Conselho Nacional de Desenvolvimento Científico e Tecnológico-Brazil), FAPESP (Fundação de Amparo à Pesquisa do Estado de São Paulo-Brazil) and DFG (Deutsche Forschungsgemeinschaft). The assistance of the IEA-R1 research reactor staff in the irradiation of the samples and of Professor Mekata, Professor Schwarzmann, and Dr. Ziegeler in the preparation of several delafossite samples is thankfully acknowledged.

*Author to whom correspondence should be addressed. Electronic address: rfranzin@net.ipen.br

¹A. Bartos, K. P. Lieb, A. F. Pasquevich, M. Uhrmacher, and ISOLDE Collaboration, *Phys. Lett. A* **157**, 513 (1991).

²A. Bartos, M. Uhrmacher, L. Ziegeler, and K. P. Lieb, *J. Alloys Compd.* **179**, 307 (1992).

³R. N. Attili, M. Uhrmacher, K. P. Lieb, L. Ziegeler, M. Mekata, and E. Schwarzman, *Phys. Rev. B* **53**, 600 (1996).

⁴D. B. Rogers, R. D. Shannon, C. T. Prewitt, and J. L. Gillson, *Inorg. Chem.* **10**, 723 (1971).

⁵M. Mekata, N. Yaguchi, T. Takagi, T. Sugino, S. Mitsuda, H. Yoshizawa, N. Hosoito, and T. Shinjo, *J. Phys. Soc. Jpn.* **62**, 4474 (1993).

⁶Y. Oohara, S. Mitsuda, H. Yoshizawa, N. Yaguchi, H. Kuriyama, T. Asano, and M. Mekata, *J. Phys. Soc. Jpn.* **63**, 847 (1994).

⁷M. Uhrmacher, R. N. Attili, K. P. Lieb, K. Winzer, and M. Mekata, *Phys. Rev. Lett.* **76**, 4829 (1996).

⁸*Table of Isotopes*, 7th ed., edited by C. M. Lederer and V. S. Shirley (Wiley, New York, 1978).

⁹E. Karlsson, E. Matthias, and K. Siegbahn, *Perturbed Angular Correlations* (North-Holland, Amsterdam, 1964).

¹⁰R. Vianden, *Hyperfine Interact.* **15/16**, 1081 (1983).

¹¹J. Luthin, K. P. Lieb, M. Neubauer, M. Uhrmacher, and B.

Lindgren, *Phys. Rev. B* **57**, 15 272 (1998).

¹²T. Ishiguro, A. Kitazawa, N. Mizutami, and M. Kato, *J. Solid State Chem.* **40**, 170 (1981).

¹³W. Dannhauser and A. P. Vaughan, *J. Am. Chem. Soc.* **77**, 896 (1955).

¹⁴C. T. Prewitt, R. D. Shannon, and D. B. Rogers, *Inorg. Chem.* **10**, 719 (1971).

¹⁵T. Ishiguro, N. Ishizawa, N. Mizutami, and M. Kato, *J. Ceram. Soc. Jpn.* **92**, 25 (1984).

¹⁶H. Haas and E. Kordes, *Z. Kristallogr.* **129**, 259 (1969).

¹⁷T. Ishiguro, N. Ishizawa, N. Mizutami, and M. Kato, *J. Solid State Chem.* **49**, 232 (1981).

¹⁸E. Gehle and H. Sabrowsky, *Z. Naturforsch. B* **30**, 659 (1975).

¹⁹B. U. Köhler and M. Jansen, *J. Solid State Chem.* **71**, 566 (1987).

²⁰F. D. Feiock and W. R. Johnson, *Phys. Rev.* **187**, 39 (1969).

²¹D. Wiarda, M. Uhrmacher, A. Bartos, and K. P. Lieb, *J. Phys.: Condens. Matter* **5**, 4111 (1993).

²²Th. Wenzel, A. Bartos, K. P. Lieb, M. Uhrmacher, and D. Wiarda, *Ann. Phys. (Leipzig)* **1**, 155 (1992).

²³J. P. Doumerc, A. Ammar, A. Wichainchai, M. Pouchard, and P. Hagenmuller, *J. Phys. Chem. Solids* **48**, 37 (1987).

²⁴R. Sternheimer, *Phys. Rev.* **130**, 1423 (1963).